Computer-aided Design/Computer-aided Manufacturing–guided Endodontic Surgery: Guided Osteotomy and Apex Localization in a Mandibular Molar with a Thick Buccal Bone Plate

So-Yeon Ahn, DDS, Nam-Hoon Kim, DDS, MSD,† Sunil Kim, DDS, MSD, PhD,* Bekir Karabucak, DMD, MS,‡ and Euiseong Kim, DDS MSD, PhD**

Abstract

A mandibular molar with a thick buccal bone plate is a challenging problem in endodontic surgery despite the increase in the success rate of endodontic surgery nowadays. This report describes the application of a surgical template to guide osteotomy and facilitate apex localization in a mandibular molar with a thick buccal bone plate. A 57-year-old woman visited the authors' clinic for pain in tooth 19 and was diagnosed with symptomatic apical periodontitis in this previously treated tooth. Nonsurgical retreatment was performed; however, 2 years later, the patient reported pain in the same tooth. A periapical lesion was confirmed using cone-beam computed tomographic (CBCT) imaging, and endodontic surgery on the mesial root of tooth 19 was planned. After CBCT imaging and cast scan data were transferred to implant surgical planning software, the data were superimposed. In the superimposed model, an anchor pin was designed to target the mesial root apex of tooth 19. The surgical template was then printed using a 3-dimensional printer. Endodontic microsurgery included application of this printed surgical template. A computer-aided design/computer-aided manufacturing (CAD/CAM)-guided surgical template minimized the extent of osteotomy and enabled precise targeting of the apex in this case. There were no postoperative complications. A CAD/CAM-guided surgical template is useful in endodontic surgery for complicated cases. *(J Endod 2018;44:665–670)*

Key Words

3D printing, apical surgery, computer-aided design/computer-aided manufacturing, endodontic surgery, surgical guide

Significance

Introducing a CAD/CAM-guided surgical template in endodontic surgery would make guided osteotomy and precise targeting of the root apex possible. The surgical template would be especially useful in performing endodontic surgery on teeth with potentially problematic anatomic structures.

Computer-aided design/computer-aided manufacturing (CAD/CAM) and 3-dimensional (3D) printing technology were first developed and applied in the late 1980s and 1990s (1). Currently, CAD/CAM and 3D printing have diverse applications in dentistry including the fabrication of dental models, temporary restorations, surgical guides for orthognathic surgery, and trays for indirect bonding of orthodontic brackets (1). Surgical guide templates using CAD/CAM and 3D printing, in particular, are commonly used in implant surgery (2). These templates have also been recently introduced in endodontic fields. Templates used in orthograde guide access cavity preparation in calcified canals (3) and guided osteotomy in endodontic surgery have been described (4, 5).

Endodontic surgery is 1 of the treatment options to manage persistent apical periodontitis after the failure of nonsurgical treatment (6). The success rate of conventional endodontic surgery is relatively low, between 43.5% and 74% (7). However, by applying contemporary techniques, including high-power magnification and illumination, microsurgical instruments, and modern filling materials (8), success rates of surgery have significantly increased, and, in turn, surgery has become a more effective treatment. Success rates for endodontic microsurgery have been reported to be between 88.9% and 100% (7).

Prognostic factors influencing endodontic surgery outcomes include lesion type, root-end filling material, and coronal restoration, among others (9). Some studies have found that tooth position also has an influence on outcome(s). In particular, the lower molars have been reported to have lower success rates than teeth in other positions. The difficulty in accessibility caused by thick buccal bone and anatomic obstacles, including the mental foramen or inferior alveolar nerve, has been attributed to poorer outcomes (10, 11).

Another factor known to be associated with improved and faster healing is the extent of periapical bony destruction (12). The extent of osteotomy also influences the degree of postoperative complications such as pain and swelling (13). However, the extent of osteotomy tends to be increased in cases with an intact buccal bone plate

From the *Microscope Center, Department of Conservative Dentistry and Oral Science Research Center, and †Department of Prosthodontics, Yonsei University College of Dentistry, Seoul, Korea; and ‡Department of Endodontics, School of Dental Medicine, University of Pennsylvania, Philadelphia, Pennsylvania.

Address requests for reprints to Dr Euiseong Kim, Department of Conservative Dentistry and Oral Science Research Center, Microscope Center, College of Dentistry, Yonsei University, 50 Yonsei-Ro, Seodaemun-Gu, Seoul, 120-752, South Korea. E-mail address: andyendo@yuhs.ac

0099-2399/$ - see front matter

https://doi.org/10.1016/j.joen.2017.12.009

because it is difficult to locate the exact location of the root apex (14). In this report, we present a method involving the application of a surgical template to guide osteotomy and facilitate precise apex localization in a case involving a thick buccal bone plate.

Case Report

A 57-year-old woman visited the clinic because of spontaneous pain in the left mandibular area. She felt tenderness to percussion on tooth 19. Periapical images revealed a periapical radiolucent lesion in the mesial root of tooth 19 (Fig. 1*A*). Periodontal probing was within normal limits. The patient reported that tooth 19 underwent root canal treatment several years previously. Given the diagnosis of symptomatic apical periodontitis in a previously treated tooth, nonsurgical retreatment was planned.

After local anesthesia with 2% lidocaine with epinephrine (1:100,000) and rubber dam application, an access cavity was prepared. A gutta-percha cone was removed using Gates-Glidden drills (Dentsply Maillefer, Ballaigues, Switzerland) and the ProTaper Universal rotary system (Dentsply Maillefer). The working length was determined using an apex locator (Root ZX; J Morita Mfg Corp, Kyoto, Japan). Additional root canal preparation was performed with the ProTaper Universal system. Irrigation was performed using 5.25% sodium hypochlorite solution. The canals were dried with sterile paper points. Obturation was performed using a continuous wave of condensation technique (System B; SybronEndo, Orange, CA) and thermoplasticized gutta-percha backfilling (Obtura III, SybronEndo). AH 26 (Dentsply Maillefer) was used as the root canal sealer.

Two years later, the patient reported bite pain in tooth 19 again. Clinical examination revealed tenderness in tooth 19 on percussion, but the tooth had normal probing depths. The remaining periapical lesion on the mesial root was confirmed on periapical radiography (Fig. 1*B*). The lesion was confirmed using cone-beam computed tomographic (CBCT) imaging (Alphrad 3030; Asahi Roentgen Ind Ltd, Kyoto, Japan), and apical surgery on the mesial root of tooth 19 was planned (Fig. 1*C* and *D*). Because the tooth had a thick and intact buccal cortical bone (Fig. 1*D* and *E*), which made exact apex localization difficult, a surgical template was designed and fabricated.

A preliminary impression was made using irreversible hydrocolloid, whereas the diagnostic cast was fabricated using yellow stone. Scanning data of the cast were generated using a blue-light benchtop 3D scanner (Identica Blue; Medit, Seoul, Korea) (Fig. 2*A*). After tooth CBCT and cast scan data were uploaded into implant surgical planning software (Ondemand3D; Cybermed Co, Seoul, Korea) (Fig. 2*B*), the data were superimposed using the In2Guide module (Cybermed Co) (Fig. 2*C*). In virtual surgical planning, an anchor pin was designed to target the mesial root apex of tooth 19, with the buccal flange extended to include the anchor pin. The guide depth was preplanned on the computer and incorporated into the stent to prevent the anchor pin from penetrating the lingual plate (Fig. 2*D*). To avoid interference with the lips and buccal cheek, the angle of the anchor pin was tilted forward approximately 30° (Fig. 2*E*). A surgical template was designed and exported in a stereolithography file format (Fig. 2*F*). This file was printed using a photopolymer printer (Object EDEN260V; Stratasys, Eden Prairie, MN). Biocompatible clear resin (MED 610, Stratasys Ltd), which

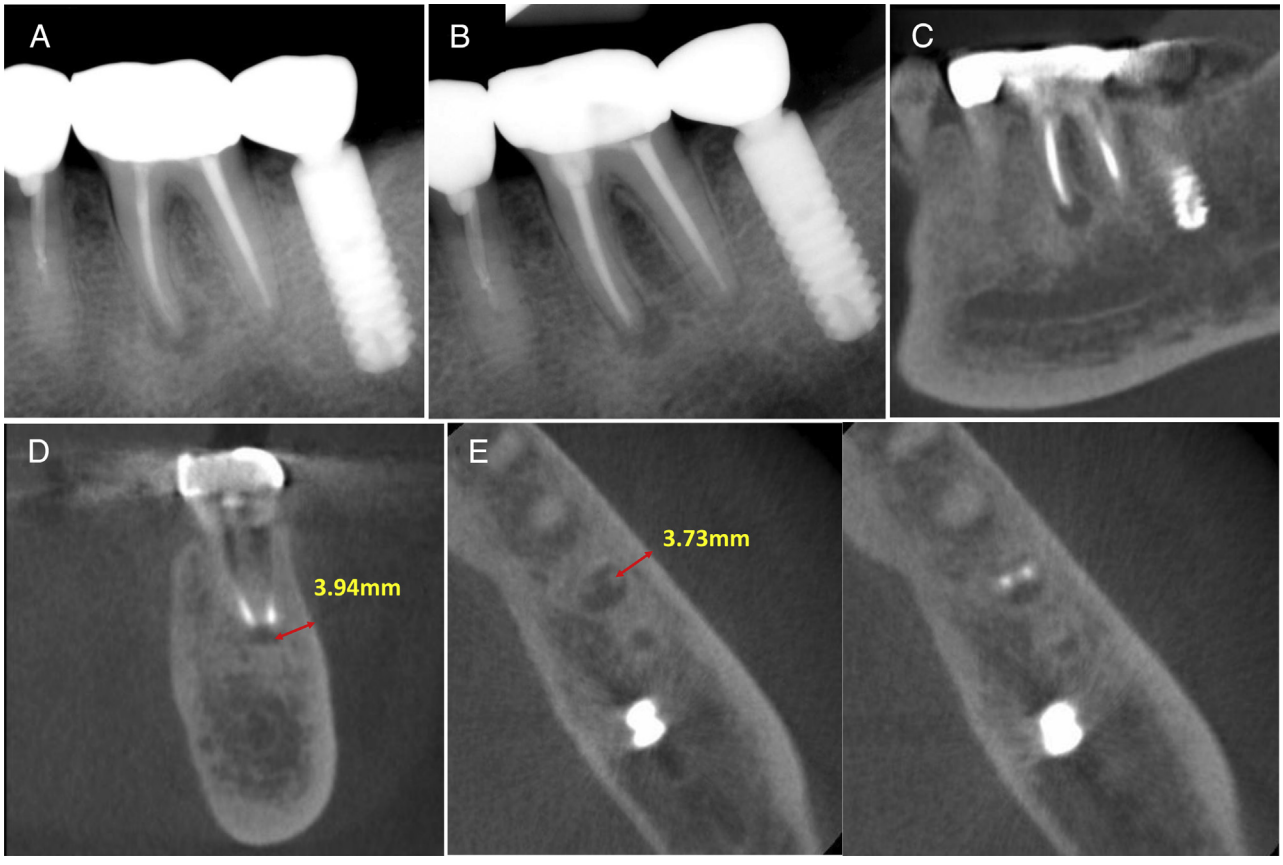

Figure 1. (*A*) The initial periapical x-ray of tooth 19 exhibiting a periapical lesion. (*B*) The periapical x-ray 2 years after nonsurgical retreatment. (*C*) A reformatted panoramic view of the CBCT scan revealing a periapical lesion in the mesial root of tooth 19. (*D*) A coronal view of the CBCT scan. A thick and intact buccal cortical bone was detected on (*E*) the axial view of the CBCT scan.

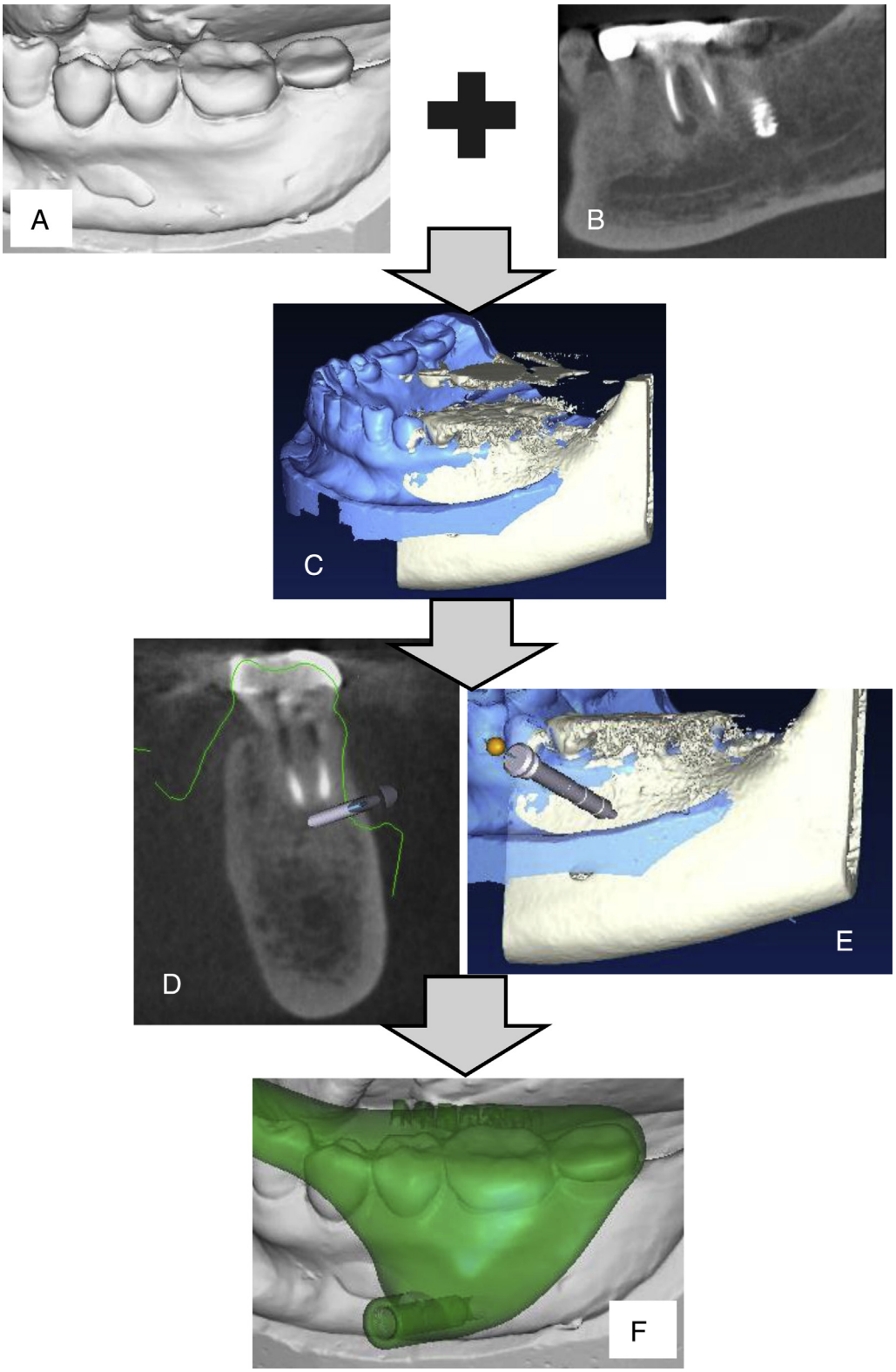

Figure 2. (*A*) Scanning data of the cast. (*B*) Tooth CBCT image uploaded into implant surgical planning software. (*C*) Superimposition of the scanned cast and the CBCT image. (*D* and *E*) The anchor pin was placed to target the mesial root apex of tooth 19. (*F*) The final design of the surgical template.

was approved in accordance with standard DIN EN ISO 10993-1:2009, was used for printing. After printing was completed, a metal sleeve was inserted (Fig. 3).

All surgical procedures were performed using a surgical operating microscope (OPMI PICO; Carl Zeiss; Göttingen, Germany). On operation day, a 3D printed surgical template was fitted on tooth 19 to verify

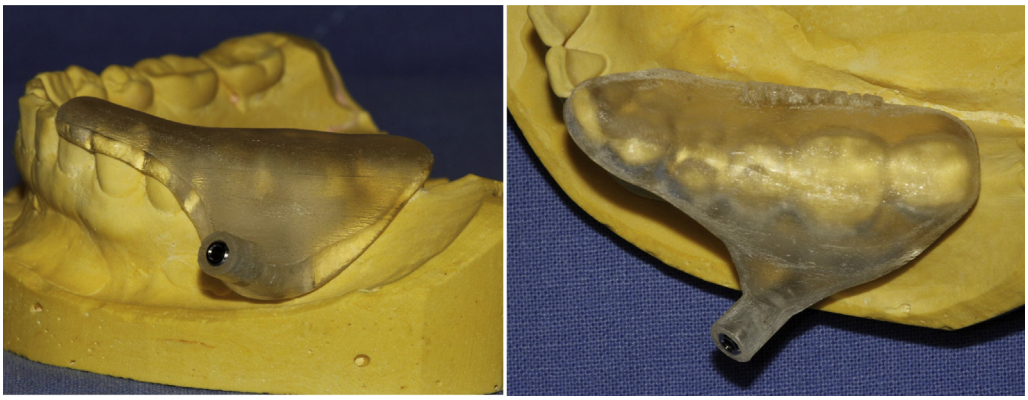

Figure 3. The 3D printed surgical template for endodontic surgery on tooth 19.

precision. The patient was anesthetized with 2% lidocaine with epinephrine (1:80,000) followed by a sulcular full-thickness flap reflection using a curette. After the surgical template was positioned on tooth 19 (Fig. 4*A*), guided osteotomy was performed using a 1.5-mm-diameter, 20-mm-long anchor drill. The surgical template was then removed, and the exposed root surface and gutta-percha cone were confirmed (Fig. 4*B*). On the coronal side of the mental foramen, a groove was made, and a KP1 retractor (G Hartzell and Son Inc, Concord, CA) was placed to protect it. Additional osteotomy was performed using a bone cutter (H161 Lindenmann; Brasseler, Savannah, GA) until sufficient space for the manipulation of ultrasonic instruments was gained (Fig. 4*C*). Periapical curettage was performed followed by 3-mm root tip resection using a 170-tapered fissure bur under copious irrigation with sterile distilled water (Fig. 4*D*). Hemostasis of the bony crypt was achieved using cotton pellets soaked with epinephrine solution (Bosmin; Jeil Pharmaceutical Co, Ltd, Seoul, Korea). The resected root surface was stained with methylene blue and inspected using a micromirror (Obtura Spartan, Fenton, MO) under 20× to 26× magnification. An isthmus was noted between the canals and was included in the design of root-end cavity preparation (Fig. 4*E*). Root-end preparation was made 3 mm into the canal space along the long axis using KIS ultrasonic tips (Obtura Spartan). The prepared root-end cavity was dried and filled with Retro MTA (BioMTA, Seoul, Korea). The adaptation of the filling material to the canal was confirmed under high magnification (20×–26×) (Fig. 4*F*). After cleaning the wound area, the flap was closed and sutured using 5-0 monofilament sutures. A postoperative radiograph was taken to verify correct root-end filling and the absence of excess material in the bony crypt (Fig. 4*H*). The sutures were removed 7 days after the operation, and there were no postoperative complications.

Discussion

Anatomic difficulties such as a thick buccal cortical bone on the mandibular raise the difficulty of endodontic surgery and lower success rates (10, 11). The buccal cortical bone in this case was intact and thick (3.73–3.94 mm according to CBCT measurement), which made it difficult to locate the root apex. Less experienced clinicians, in particular, can mistakenly perform excessive osteotomy in such cases (14). In this case, a 3D printed surgical template was applied for guided osteotomy and precise apex targeting. The diameter of the bony crypt in this case was 4 mm (Fig. 4*G*), which was a suitable minimum required access for instrument manipulation (15).

The diameter of a bony defect influences healing outcome(s) after endodontic surgery. Extensive bone destruction tends to result in uncertain or unsuccessful healing, delays in the healing process (12, 16), and risk for postoperative complications. Surgical trauma, including osteotomy, initiates the inflammatory process, which leads to postoperative complications including pain and swelling (13). Decreasing the extent of osteotomy can help reduce surgical complications and promote healing. Therefore, guided osteotomy using a 3D printed surgical template can in theory decrease postoperative complications and enhance healing.

Although 3D fabrication of surgical templates is a time-consuming process (5), the length of the surgical procedure itself can be decreased. By applying a surgical template in this case, the root tip was exposed immediately after removing the buccal bone plate in this case and, moreover, obviated the need to search for the root apex. Because the degree of postoperative swelling is known to be influenced by the length of the surgical procedure, strategies to reduce duration are a valid goal toward reducing discomfort in patients during the healing period (17).

Surgical templates are particularly helpful in difficult cases involving teeth near potentially problematic anatomic structures. Structures such as adjacent root tips, the inferior alveolar nerve, the mental foramen, and the maxillary sinus contribute to difficulty in surgical approaches to the root apex (4). However, guided surgery (avoiding anatomic landmarks) can be achieved using a surgical template. This means that a CAD/CAM-guided surgical template may broaden the indications for endodontic microsurgery.

To manufacture an accurate surgical template, proper case selection and delicate design are necessary. Scattering in CBCT images, originating from metallic restorations, may cause inaccurate superimposition with scanned stone models. Thus, the accuracy of the surgical template is limited in patients with several metallic prostheses (18). Clinicians may forego surgical templates in these cases or consider artificial landmarks to overcome this limitation (19). In fact, there were many prostheses generating artifacts in the present case (Fig. 2*C*). Fortunately, there was a natural tooth (tooth 21) in this case that made superimposition possible. Additionally, a delicate design process is needed to precisely target the anchor pin to the root apex while avoiding the lips and cheeks.

Within the limitations of this study, introducing a CAD/CAM-guided surgical template in endodontic surgery helps to minimize the extent of osteotomy and facilitates locating the root apex in cases with a thick and intact buccal bone plate. The surgical template would be useful in apical surgery on teeth with problematic anatomic structures. Additionally, surgical time would decrease by the diminished time consumed to search for the root apex although the preparation time for surgery might be increased because designing and fabricating surgical stents take

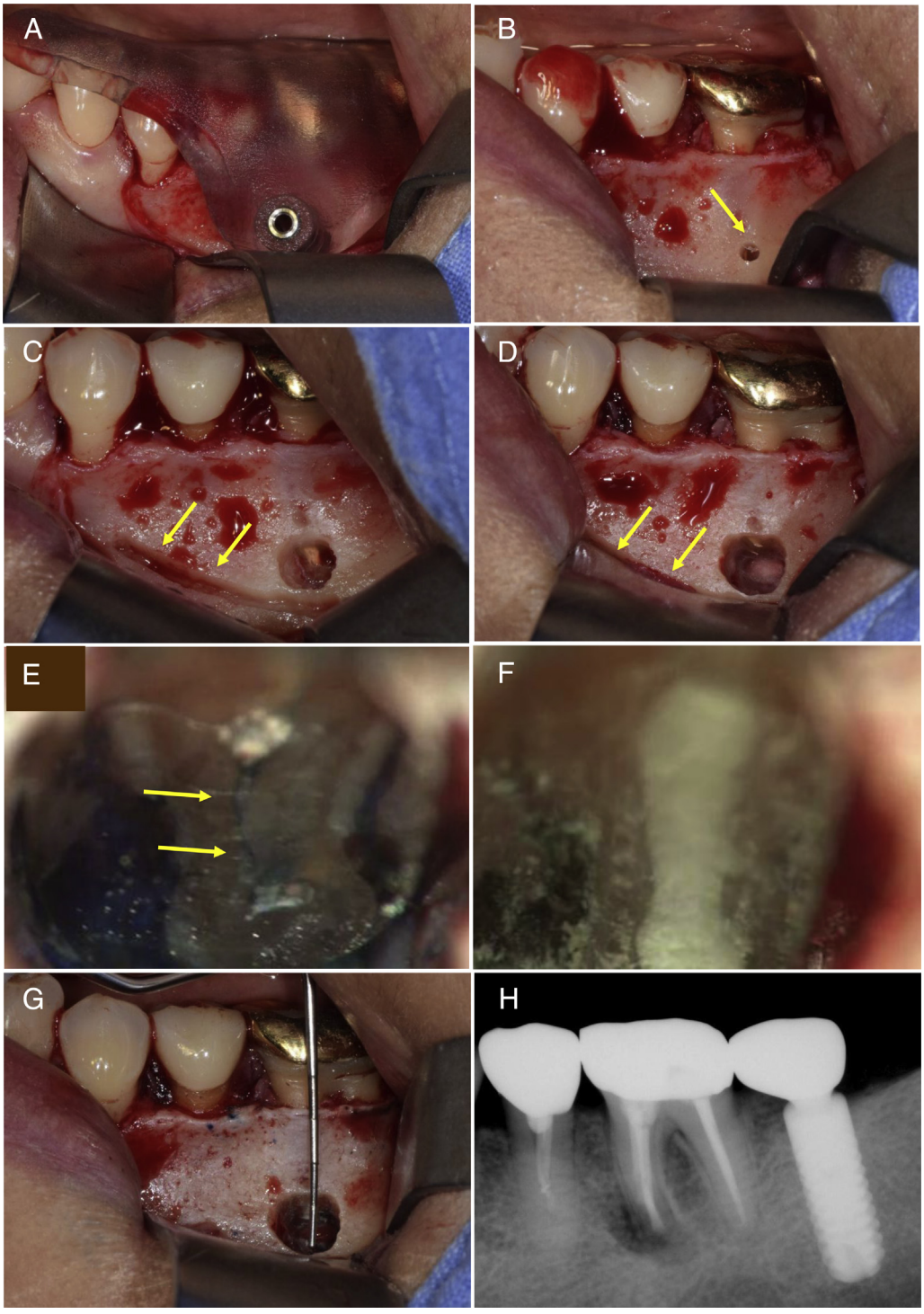

Figure 4. (*A*) The surgical template was positioned on tooth 19. (*B*) After drilling using an anchor drill, exposure of the root tip (*yellow arrow*) was confirmed. (*C*) The bony crypt was enlarged to enable instrument manipulation. A groove (*yellow arrow*) was made on the coronal side of a mental foramen to protect it. (*D*) The bony crypt after root resection. A KP1 retractor was placed on the groove (*yellow arrow*). (*E*) The resected root surface inspected under high magnification. The isthmus between the mesiobuccal and mesiolingual canal was inspected (*yellow arrow*). (*F*) Root-end filling with Retro MTA was confirmed under high magnification. (*G*) The diameter of the bony crypt after surgery was 4 mm. (*H*) The postoperative periapical x-ray image.

time. Nevertheless, proper case selection and a delicate design process are necessary for producing an effective surgical template.

Acknowledgments

So-Yeon Ahn and Nam-Hoon Kim contributed equally to this study.

Supported by the Basic Science Research Program through the National Research Foundation of Korea funded by the Ministry of Education (grant no. 2015R1D1A1A09057552).

The authors deny any conflicts of interest related to this study.

References

1. Dawood A, Marti Marti B, Sauret-Jackson V, Darwood A. 3D printing in dentistry. Br Dent J 2015;219:521–9.
2. Jung RE, Schneider D, Ganeles J, et al. Computer technology applications in surgical implant dentistry: a systematic review. Int J Oral Maxillofac Implants 2009; 24(Suppl):92–109.
3. Zehnder MS, Connert T, Weiger R, et al. Guided endodontics: accuracy of a novel method for guided access cavity preparation and root canal location. Int Endod J 2016;49:966–72.
4. Pinsky HM, Champleboux G, Sarment DP. Periapical surgery using CAD/CAM guidance: preclinical results. J Endod 2007;33:148–51.
5. Strbac GD, Schnappauf A, Giannis K, et al. Guided modern endodontic surgery: a novel approach for guided osteotomy and root resection. J Endod 2017;43: 496–501.
6. Karabucak B, Setzer F. Criteria for the ideal treatment option for failed endodontics: surgical or nonsurgical? Compend Contin Educ Dent 2007;28:391–7;quiz 398, 407.
7. Setzer FC, Shah SB, Kohli MR, et al. Outcome of endodontic surgery: a meta-analysis of the literature–part 1: comparison of traditional root-end surgery and endodontic microsurgery. J Endod 2010;36:1757–65.
8. Kim S, Kratchman S. Modern endodontic surgery concepts and practice: a review. J Endod 2006;32:601–23.
9. Song M, Kim SG, Lee SJ, et al. Prognostic factors of clinical outcomes in endodontic microsurgery: a prospective study. J Endod 2013;39:1491–7.
10. Zhou W, Zheng Q, Tan X, et al. Comparison of mineral trioxide aggregate and iRoot BP Plus Root Repair Material as root-end filling materials in endodontic microsurgery: a prospective randomized controlled study. J Endod 2017;43:1–6.
11. Kim S, Jung H, Kim S, et al. The influence of an isthmus on the outcomes of surgically treated molars: a retrospective study. J Endod 2016;42:1029–34.
12. von Arx T, Hanni S, Jensen SS. Correlation of bone defect dimensions with healing outcome one year after apical surgery. J Endod 2007;33:1044–8.
13. Sisk AL, Hammer WB, Shelton DW, Joy ED Jr. Complications following removal of impacted third molars: the role of the experience of the surgeon. J Oral Maxillofac Surg 1986;44:855–9.
14. Gutmann JL, Harrison JW. Posterior endodontic surgery: anatomical considerations and clinical techniques. Int Endod J 1985;18:8–34.
15. Abedi HR, Van Mierlo BL, Wilder-Smith P, Torabinejad M. Effects of ultrasonic root-end cavity preparation on the root apex. Oral Surg Oral Med Oral Pathol Oral Radiol Endod 1995;80:207–13.
16. Song M, Kim SG, Shin SJ, et al. The influence of bone tissue deficiency on the outcome of endodontic microsurgery: a prospective study. J Endod 2013;39: 1341–5.
17. Capuzzi P, Montebugnoli L, Vaccaro MA. Extraction of impacted third molars. A longitudinal prospective study on factors that affect postoperative recovery. Oral Surg Oral Med Oral Pathol 1994;77:341–3.
18. Mora MA, Chenin DL, Arce RM. Software tools and surgical guides in dental-implant-guided surgery. Dent Clin North Am 2014;58:597–626.
19. Kim JE, Amelya A, Shin Y, Shim JS. Accuracy of intraoral digital impressions using an artificial landmark. J Prosthet Dent 2017;117:755–61.